Carbohydrate Polymers 110 (2014) 95–99

Contents lists available at ScienceDirect

Carbohydrate Polymers

journal homepage: www.elsevier.com/locate/carbpol

Short communication

Injectable hyaluronic acid hydrogel for ^{19}F magnetic resonance imaging

Xia Yang [a], Yi Sun [b,c], Sujit Kootala [a], Jöns Hilborn [a], Arend Heerschap [b], Dmitri Ossipov [a,*]

[a] Department of Chemistry-Angstrom, Uppsala University, Uppsala, Sweden
[b] Department of Radiology, Radboud University Nijmegen Medical Centre, Nijmegen, The Netherlands
[c] Department of Urology, Radboud University Nijmegen Medical Centre, Nijmegen, The Netherlands

ARTICLE INFO

Article history:
Received 18 October 2013
Received in revised form 28 February 2014
Accepted 20 March 2014
Available online 2 April 2014

Keywords:
Hyaluronan
Hydrogel
Injectable
^{19}F MRI
Chemoselective reactions

ABSTRACT

We report on a ^{19}F labeled injectable hyaluronic acid (HA) hydrogel that can be monitored by both ^{1}H and ^{19}F MR imaging. The HA based hydrogel formed *via* carbazone reaction can be obtained within a minute by simple mixing of HA-carbazate and HA-aldehyde derivatized polymers. ^{19}F contrast agent was linked to with carbazate and thiol dually functionalized HA *via* orthogonal Michael addition reaction which afforded cross-linkable and ^{19}F labeled HA. The ^{19}F labeling of HA polymer did not affect the mechanical properties of the formed hydrogel. As a result, the shape of a hydrogel sample could be imaged very well by both ^{1}H MRI and high resolution ^{19}F MRI. This hydrogel has high potential in clinical applications since it is injectable, biocompatible, and can be tracked in a minimally invasive manner. The present approach can be applied in preparation of injectable ^{19}F labeled hydrogel biomaterials from other natural biomacromolecules.

1. Introduction

Magnetic resonance imaging (MRI) is a non-invasive, radiation-free, high-resolution imaging technique. It is widely applied in clinical diagnostics and research, including tissue engineering (Nitzsche et al., 2009). Using MRI, researchers could track bone (Hartman et al., 2002) or soft tissue formation continuously *in vivo* (Neves, Medcalf, & Brindle, 2003). Changes in MR parameters such as T_1, T_2 relaxation times and diffusion coefficients reflect changes in material properties (Cheng, Loai, & Farhat, 2012; Reiter et al., 2012). Contrast agents that affect local water relaxation rates can improve the visibility of MR images. But, due to the great amount of protons in the background (organs, blood, body fluid, *etc.*), proton based contrast agents often lack specificity as interpretation of MR images may be obscured. Hence, hetero-nuclear MRI, such as ^{19}F MRI (Morawski et al., 2004; Srinivas, Heerschap, Ahrens, Figdor, & Vries, 2010), which has better contrast and higher specificity, becomes attractive. Many ^{19}F-containing compounds have been developed as contrast agents to track materials by ^{19}F MRI (Oishi, Sumitani, & Nagasaki, 2007; Senanayake, Kenwright, Parker, & Hoorn, 2007). The 100% naturally abundant ^{19}F nucleus has an MR sensitivity almost as high as for protons, but with nearly no endogenous background resulting into a high specificity of ^{19}F MRI. Additionally, under ideal circumstances, the signal intensity of ^{19}F is directly related to its concentration and enables quantitative measurements over time (Srinivas et al., 2010; Srinivas, Morel, Ernst, Laidlaw, & Ahrens, 2007).

In our previous studies, we developed injectable hydrogels based on multifunctional hyaluronic acid (HA) that can be used for drug delivery (Ossipov, Yang, Varghese, Kootala, & Hiborn, 2010) or tissue regeneration (Yang et al., 2012). HA polymer is the main component of extracellular matrix (ECM) and it plays an important role in regenerating various tissues such as bone, cartilage and can stimulate angiogenesis. It can also interact specifically with tumor cells that over-express the HA receptor CD44 (Ossipov, Kootala, Yi, Yang, & Hilborn, 2013). Therefore, it is important to be able to map the distribution of this material and understand its behavior *in vitro* and *in vivo*. MRI provides the possibility to monitor the hydrogel without interfering with experimental process. It is a challenge to investigate the location and shape of hydrogels correctly by only ^{1}H MRI, because of background signals by the large amount of body protons and the abundant water content of hydrogel material (~98%, w/v). To tackle this problem, in this study, we introduced a ^{19}F group to HA-based material. This injectable hydrogel is particularly useful in clinical applications since it can be administered and subsequently tracked *in vivo* in a minimally invasive manner

* Corresponding author at: Department of Chemistry-Angstrom, Uppsala University, Uppsala SE 751 21, Sweden. Tel.: +46 18 471 7335; fax: +46 18 471 3477.
E-mail addresses: dmitri.ossipov@kemi.uu.se, dmitri.ossipov@mkem.uu.se (D. Ossipov).

http://dx.doi.org/10.1016/j.carbpol.2014.03.070
0144-8617/

(*i.e.* with no need to sacrifice animals). Moreover, the change in ^{19}F signal intensity allows to monitor hydrogel material after injection with high imaging specificity and to quantify the gel degradation. The present *in vivo* injectable approach to incorporation a fluorine imaging agent without the need for hydrogel purification can also be easily applied to other hydrogel-based biomaterials.

2. Experimental

2.1. Materials

1,1′-Carbonyldiimidazole (CDI), serine methyl eater hydrochloride, 1,3-dioxan-2-one, DL-dithiothreitol (DTT), hydrazine, N-hydroxybenzotriazole (HOBt), 1-ethyl-3-(3-dimethylaminopropyl)carbodiimide (EDC), and 2,2′-dithiobisethanol **1** were purchased from Aldrich Chemical Co. Hyaluronic acid (HA) sodium salt of the molecular weight 59 kDa was purchased from Lifecore Biomedical. 2,2′-dithiobisethanol **1** was purchased from Fluka. HA-aldehyde (HA-al) was synthesized according to the literature procedures (Ossipov et al., 2010). All solvents were of analytical quality (p.a.) and were dried over 4 Å molecular sieves. Dialysis membranes Spectra/Por 6 (3500, g/mol cut off) were purchased from VWR International. The NMR experiments were carried out on Jeol JNM-ECP Series FT NMR system at a magnetic field strength of 9.4 T, operating at 400 MHz for ^{1}H and ^{19}F. Details of chemical synthesis and cytotoxicity experiments were described in Supporting Information.

2.2. Preparation and characterization of hydrogel

5 mg of HA-carb-^{19}F polymer was dissolved in 250 μl of PBS buffer. Meanwhile, 5 mg of HA-al polymer was dissolved in 250 μl of PBS buffer separately. Two polymer solutions were mixed in the syringe and sealed with Para-film for 2 h before further using. Control hydrogel was prepared by mixing HA-carb polymer (without ^{19}F modification) with HA-al polymer at the same concentration. The final concentration was 2% (w/v) for all hydrogel samples. Rheological characterizations of all hydrogels were performed using an AR2000 Advanced Rheometer (TA Instruments) with an aluminium parallel plate geometry of 8 mm diameter. The total volume of tested material was 0.15 ml. Strain sweeps were performed by monitoring storage (G′) and loss moduli (G″) at a fixed normal force (0.05 N), gap (1000) and a fixed frequency (1 Hz) as a function of % strain between 1 and 500. All experiments were repeated three times. After rheology tests, the samples were immerged into 2 ml

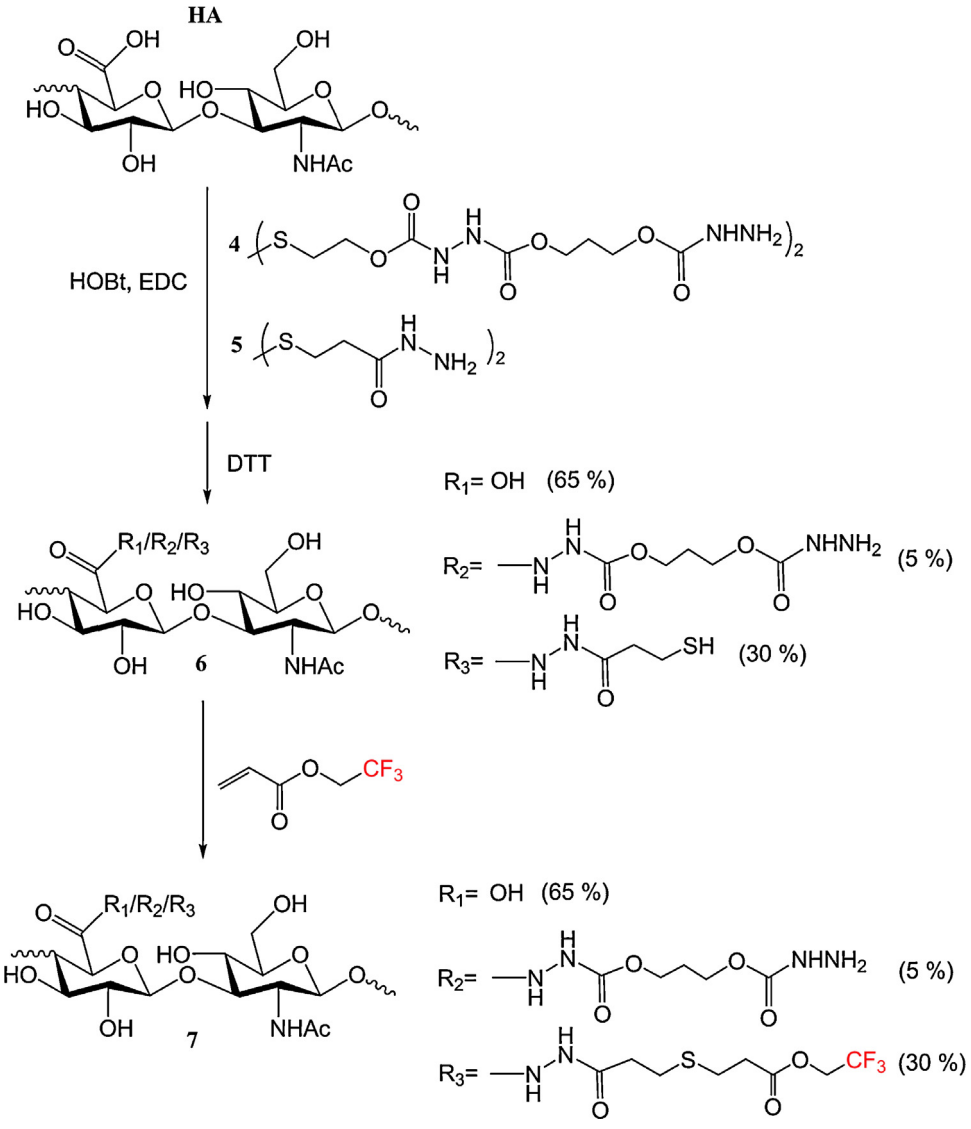

Fig. 1. Synthesis of HA polymer dually functionalized with a carbazate group and a ^{19}F-label (HA-carb-^{19}F).

of PBS buffer (10 mM, pH 7.4) for 24 h swelling ratio measurement. The swelling ratio (%) was calculated according to the weight difference before (W_0) and after (W_t) swelling in PBS buffer: swelling ratio = $((W_t - W_0) \times 100)/W_0$. In order to investigate the elements of hydrogels, we performed Scanning electron microscope-Energy dispersive X-ray spectroscopy (SEM-EDS) mapping (SEM, LEO 1550, Zeiss). All samples were coated with 8–10 nm of Au/Pd after freeze-drying. EDS was performed at acc. voltage 5 keV.

2.3. MRI experiments

100 μl of ^{19}F-labeled HA hydrogel was put into a 1 ml Eppendorf for the MR imaging. MRI was performed on a 7T animal system (Clinscan, Bruker), using a ^{1}H–^{19}F two-channel home-built solenoid coil. ^{1}H image was acquired with 2D gradient echo sequence, with field of view (FOV) = 60 mm × 60 mm, matrix size = 128 × 128, slice thickness = 20 mm, repetition time (TR) = 100 ms, Echo time (TE) = 10 ms. Total acquisition time = 13 s. ^{19}F images were acquired using the same sequence, slice thickness and FOV. The low resolution ^{19}F images with a matrix size of 32 × 32, acquired with TE = 1.2 ms, TR = 88 ms, 4 averages, the scan is 12 min 3 s. While the high resolution ^{19}F image using TE = 1.4 ms, TR = 500 ms, matrix size 64*64, 64 averages, the total acquisition time is 18 h 16 min.

3. Results and discussion

3.1. Preparation of functionalized HA polymers

We simultaneously functionalized HA with both carbazate groups for injectable hydrogel formation and thiol groups for ^{19}F modification to give polymer **6** (Fig. 1). The mechanism of the dual modification was similar to our previously reported simultaneous incorporation of hydrazide and thiol group *via* a 2,2′-dithiobis(ethoxycarbonyl) divalent protection group (Ossipov et al., 2010). Here, linker **4** (see Supporting Information (SI) for the synthesis details) was designed to couple with HA carboxyl groups *via* amidation reaction. After amide coupling, carbazate group was generated by dithiothreitol (DTT) initiated cleavage of the disulfide bond of the linker. Finally, Michael addition of thiol group of **6** to acrylate group of trifluoroethyl acrylate afforded HA-carb-^{19}F **7** (Fig. 1). ^{1}H NMR spectroscopy confirmed the dual modification of HA **7** with a carbazate group and a ^{19}F label (Fig. 2a). Peaks α, β and γ corresponded to sixmethylene protons of the carbazate side chain, while peaks 1 and 2 corresponded to four protons of the thiol side chain. Peaks 3, 4, and 5 were assigned to the protons of the attached ^{19}F ligand. Notably, quartet of protons of CH_2-CF_3 fragment at 4.6 ppm had a characteristic $^{3}J_{H-F}$ constant of 8.8 Hz. ^{1}H–^{19}F heteronuclear coupling was also confirmed in a 2D NMR experiment (Fig. S1 of SI). Basing on integration of the corresponding ^{1}H NMR signals, we calculated that the molar ratio of thiol groups to HA disaccharide units (degree of substitution) was 30%, while the degree of carbazate substitution was 5%. This implies that all thiol groups were modified with ^{19}F label after Michael addition reaction. A singlet at −73.4 ppm obtained from ^{19}F NMR also supported successful linkage of ^{19}F the HA polymer (Fig. 2b).

3.2. Preparation and characterization of ^{19}F-labeled hydrogel

^{19}F-labeled hydrogel was prepared by simple mixing of aqueous solutions of HA-aldehyde (HA-al) and HA-carbazate-^{19}F derivatives as a result of carbazone coupling reaction (Fig. 3a). HA hydrogel (HA-al + HA-carb) without ^{19}F label was also prepared as a control to investigate the effect of linking of ^{19}F imaging agent on hydrogel properties. The "click" reaction between carbazate and aldehyde group is rapid so that both hydrogels can form within a minute.

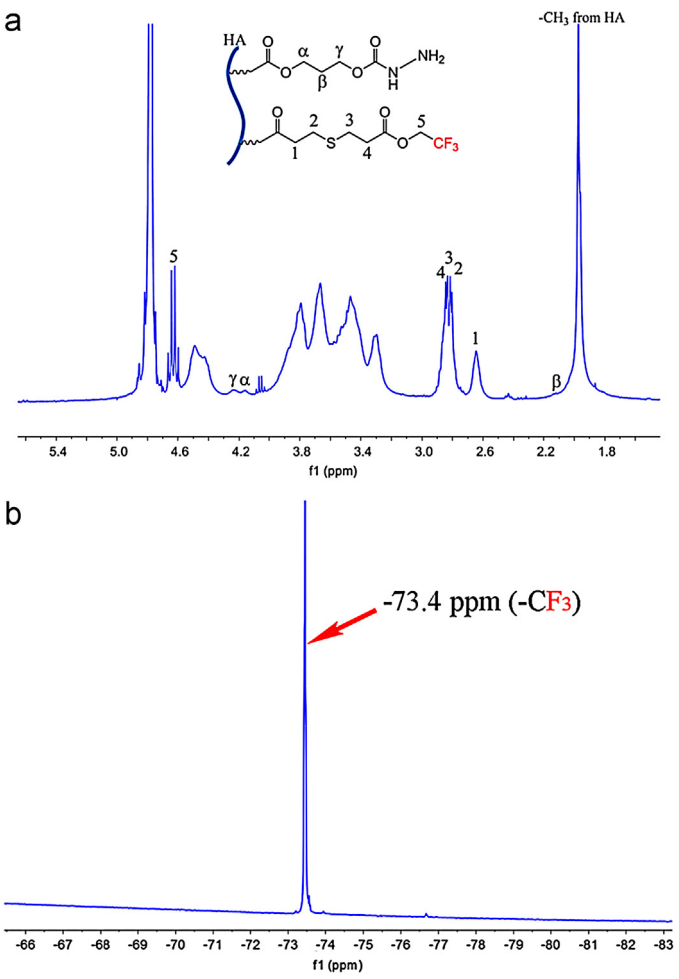

Fig. 2. ^{1}H NMR (a) and ^{19}F NMR (b) spectra of HA-carb-^{19}F.

From scanning electron microscope-energy dispersive X-ray spectroscopy (SEM-EDS, Fig. 3b), fluorine signal was found at 0.2 keV and it was homogenously distributed in the hydrogel matrix. In contrast, we did not find any fluorine signal in SEM-EDS images of the unlabeled HA hydrogel (Fig. S2). Based on the degree of fluorination in HA-carb-^{19}F, the amount of fluorine per solid content of the hydrogel was calculated to be 1.9% (w/w). As the ^{19}F signal intensity in ^{19}F MR images is proportional to ^{19}F concentration (Morawski et al., 2004), it should be possible to track the material *in vivo* by ^{19}F MRI. Rheological data showed that linking of ^{19}F group had a negligible influence on the mechanical properties of the HA hydrogel (Fig. 3c). The storage modulus (G′) of the ^{19}F-labeled HA hydrogel was 458 ± 13 Pa (n = 3, frequency = 1 Hz, % strain = 4) which was not significantly different from the G′ of the unlabeled HA hydrogel (447 ± 21 Pa). Critical strain amplitude occurred at % strain 100, and G′ started to decrease at % strain 200 for both hydrogels. The degree of substitution with carbazate (5%) and molecular weight (59 kDa) were the same for both HA polymers (HA-carb-^{19}F and HA-carb). It appeared that modification with ^{19}F groups does not result in additional physical association between the modified groups. Thus, the mechanical property of the ^{19}F-labeled HA hydrogel are expected to be the same as for the unlabeled hydrogel. On the other hand, we found that HA-^{19}F hydrogel showed lower swelling ratio (127 ± 5%) as compared with the un-modified HA hydrogel (215 ±15%) after swelling in PBS for 24 h. Since only 65% of carboxyl group was remained in HA-carb-^{19}F polymer, while 95% of carboxyl group was still remained in HA-carb polymer, the ionic repulsion between negatively charged carboxyl group is expected

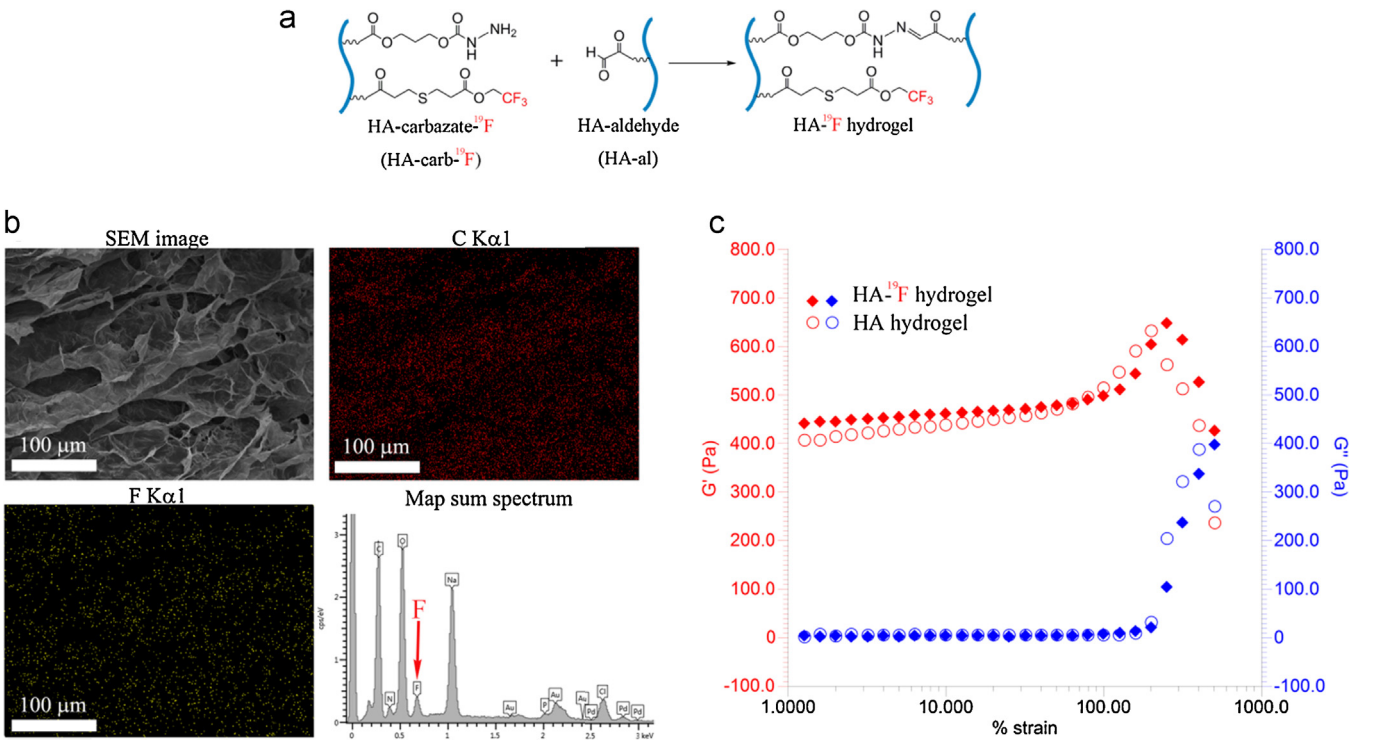

Fig. 3. (a) Formation of injectable ^{19}F-labeled hydrogel by mixing HA-carb-^{19}F and HA-al. (b) SEM-EDS mapping of HA-carb-^{19}F hydrogel. (c) Strain sweep measurement of HA-^{19}F hydrogel and unmodified HA hydrogel.

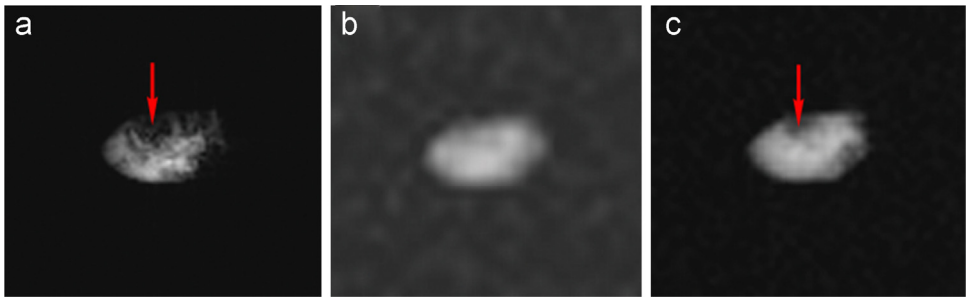

Fig. 4. MR image of ^{19}F-labeled HA hydrogel in an Eppendorf tube. (a) ^{1}H image (acquisition time TA = 13 s), (b) ^{19}F image (TA = 12 min 3 s), (c) high resolution ^{19}F image with more averages (TA = 18 h 16 min 38 s). (For interpretation of the references to color in the text, the reader is referred to the web version of the article.)

to be higher in the unmodified HA hydrogel resulting in higher swelling ratio. Finally, we found that the hydrogel forming HA derivatives as well as their degradation products are not toxic to pre-osteoblastic cells at concentration up to 0.1 mg/mL (Fig. S4).

3.3. MRI

A single peak with high signal to noisy ratio was found in ^{19}F MR spectra of the HA-^{19}F hydrogel (Fig. S3) demonstrating its great capability for ^{19}F MR imaging. In ^{1}H MR images, the shape of the hydrogel was clearly visible as a hyperintense region (Fig. 4a). The hypointense spot (red arrow) was due to an air bubble formed inside the hydrogel during mixing and injection of the hydrogel. The hydrogel could also be observed by ^{19}F MRI (Fig. 4b) as a hyperintense region, and it reflected the shape of the material that contained the ^{19}F probe. Higher resolution ^{19}F MR images obtained with more averages showed more details such as the air bubble inside (red arrow, Fig. 4c), which is consistent with the ^{1}H images.

4. Conclusion

In conclusion, we have successfully developed an injectable ^{19}F-labeled HA hydrogel that can be observed by both ^{1}H and ^{19}F MRI. The ^{1}H and ^{19}F images of the ^{19}F-labeled HA hydrogel were in good agreement to each other. This hydrogel is based on biocompatible HA polymer that can be used in clinical applications for drug delivery and tissue regeneration. This labeling strategy can also be transferred to other hydrogels in order to track this material by MRI *in vitro* and *in vivo*.

Acknowledgment

This research has received funding from the European Community's Seventh Framework Programme MultiTERM (grant agreement nr 238551).

Appendix A. Supplementary data

Supplementary data associated with this article can be found, in the online version, at http://dx.doi.org/10.1016/j.carbpol.2014.03.070.

References

Cheng, H. M., Loai, Y., & Farhat, W. A. (2012). Monitoring tissue development in a cellular matrix-based regeneration for bladder tissue engineering: Multiexponential diffusion and T_2 for improved specificity. *NMR in Biomedicine*, *25*, 418–426.

Hartman, H. M., Pikkemaat, J. A., Vehof, J. W. M., Heerschap, A., Jansen, J. A., & Spauwen, P. H. M. (2002). In vivo magnetic resonance imaging explorative study of ectopic bone formation in the rat. *Tissue Engineering*, *8*, 1029–1036.

Morawski, A. M., Winter, P. M., Yu, X., Fuhrhop, R. W., Scott, M. J., Hockett, F., et al. (2004). Quantitative magnetic resonance immunohistochemistry with ligand-targeted ^{19}F nanoparticles. *Magnetic Resonance in Medicine*, *52*, 1255–1262.

Neves, A. A., Medcalf, N., & Brindle, K. (2003). Functional assessment of tissue-engineered meniscal cartilage by magnetic resonance imaging and spectroscopy. *Tissue Engineering*, *9*, 51–62.

Nitzsche, H., Metz, H., Lochmann, A., Bernstein, A., Hause, G., Groth, T., et al. (2009). Characterization of scaffolds for tissue engineering by benchtop-magnetic resonance imaging. *Tissue Engineering Part C: Methods*, *15*, 512–521.

Oishi, M., Sumitani, S., & Nagasaki, Y. (2007). On-off regulation of ^{19}F magnetic resonance signals based on pH-sensitive PEGylated nanogels for potential tumor-specific smart ^{19}F MRI probes. *Bioconjugate Chemistry*, *18*, 1379–1382.

Ossipov, D., Kootala, S., Yi, Z., Yang, X., & Hilborn, J. (2013). Orthogonal chemoselective assembly of hyaluronic acid networks and nanogels for drug delivery. *Macromolecules*, *46*, 4105–4113.

Ossipov, D. A., Yang, X., Varghese, O., Kootala, S., & Hiborn, J. (2010). Modular approach to functional hyaluronic acid hydrogels using orthogonal chemical reactions. *Chemical Communications*, *46*, 8368–8370.

Reiter, D. A., Irrechukwu, O., Lin, P., Moghadam, S., Thaer, S. V., Pleshko, N., et al. (2012). Improved MR-based characterization of engineered cartilage using multiexponential T_2 relaxation and multivariate analysis. *NMR in Biomedicine*, *25*, 476–488.

Senanayake, P. K., Kenwright, A. M., Parker, D., & Hoorn, S. K. (2007). Responsive fluorinated lanthanide probes for ^{19}F magnetic resonance spectroscopy. *Chemical Communications*, *28*, 2923–2925.

Srinivas, M., Heerschap, A., Ahrens, E. T., Figdor, C. G., & Vries, I. J. M. (2010). ^{19}F MRI for quantitative in vivo cell tracking. *Trends in Biotechnology*, *28*, 363–370.

Srinivas, M., Morel, P. A., Ernst, L. A., Laidlaw, D. H., & Ahrens, E. T. (2007). Fluorine-19 MRI for visualization and quantification of cell migration in a diabetes model. *Magnetic Resonance in Medicine*, *58*, 725–734.

Yang, X., Akhtar, S., Rubino, S., Leifer, K., Hilborn, J., & Ossipov, D. (2012). Direct click synthesis of hybrid bisphosphonate-hyaluronic acid hydrogel in aqueous solution for biomineralization. *Chemistry of Materials*, *24*, 1690–1697.